Journal of Applied Polymer Science

Microintumescent mechanism of flame-retardant water-based chitosan–ammonium polyphosphate multilayer nanocoating on cotton fabric

Maude Jimenez,[1] Tyler Guin,[2] Severine Bellayer,[1] Renaud Dupretz,[1] Serge Bourbigot,[1] Jaime C. Grunlan[2]

[1]Unité Matériaux Et Transformations Team Reaction and Resistance to Fire (UMET-ISP-R2FIRE), Lille University, ENSCL, CS90108, Villeneuve D'Ascq F-59652, France

[2]Department of Mechanical Engineering, Texas A&M University, College Station, Texas 77843-3123

Correspondence to: M. Jimenez (E-mail: maude.jimenez@univ-lille1.fr) and J. C. Grunlan (E-mail: jgrunlan@tamu.edu)

ABSTRACT: Layer-by-layer (LbL) assembly of nanocoatings on fabric substrates has been very successful in terms of reduction of flammability. In particular, an LbL system comprised ammonium polyphosphate as the polyanion and chitosan as the polycation, applied to cotton fabric, dramatically reduced cotton flammability. At this point, the fire-retardant (FR) mechanism of action of this system has never been fully elucidated. Sonicated and nonsonicated coated cotton fabrics were evaluated using a vertical flame test and mass loss calorimeter. Coating morphology was investigated before and after burning. Thermal analyses and chemical analyses in the condensed phase (and in the gas phase) were conducted to reveal the FR mechanism of action. At the cotton surface, a combination of both condensed (formation of aromatic char) and gas phase (release of water and highly flammable gases) mechanisms impart the FR behavior, promoting a kind of "microintumescence" phenomenon. © 2016 Wiley Periodicals, Inc. J. Appl. Polym. Sci. **2016**, *133*, 43783.

KEYWORDS: cellulose and other wood products; coatings; degradation; flame retardance; polyelectrolytes

Received 26 February 2016; accepted 11 April 2016
DOI: 10.1002/app.43783

INTRODUCTION

In recent years, layer-by-layer (LbL) deposition has proven to be an efficient and versatile means for depositing functional polymer coatings on surfaces. This deposition technique consists of alternating exposure of aqueous polyanions and polycations to a solid substrate, leading to the formation of polyelectrolyte multilayer films. LbL assembly mainly involves noncovalent interactions, such as electrostatic forces, hydrogen bonding, molecular recognition, and charge–transfer interaction. It has generated great interest in many research fields, leading to the improvement of gas barrier,[1–14] antimicrobial,[15–20] antireflective,[21–26] and many other properties of textiles and other polymeric substrates.[27–30] Of particularly high impact are the studies that have used LbL nanocoatings to decrease the flammability of various substrates, such as cellulose fibers,[31–43] using environmentally benign ingredients. Various systems have been developed for cotton fabric, such as phosphonated oligoallylamines,[43] chitosan (CH)-poly(sodium phosphate) (PSP),[34] CH-ammonium polyphosphate (APP),[35] and silica-APP.[44] More recent work has focused on improving the industrial feasibility of the LbL process, for example, by spraying the coating instead of dipping,[45–53] or by using a continuous dipping procedure akin to the padding process used in the textile industry.[54,55] Additionally, an ultrasonication rinsing step between each deposition step was shown to improve the hand of cotton treated with a CH–PSP system and it also reduced the weight gain necessary to pass a vertical flame test.[34]

Previous work on LbL-assembled flame-retardant (FR) systems report very interesting results in terms of low flammability, but the mechanism of action of these systems has never been fully elucidated. An initial mechanistic explanation was recently proposed for a poly(allylamine HCl)–montmorrilonite clay system applied to a nylon film,[56] but no similar work has been published with regard to cotton fabric coated with only polymers (i.e., no clay or other inorganic materials). In this study, an LbL system comprised APP as the polyanion and CH as the polycation, was applied to cotton fabric. In this case, APP can act as an acid source, reacting with the cotton substrate to form an intumescent FR. CH is an environmentally benign and carbon-rich polymer which can serve as a carbon source in an

Additional Supporting Information may be found in the online version of this article.

intumescent system.[35] The aim of this article is to provide evidence for the mechanism of FR action, which does not appear to be classical intumescence. The full mechanism of action of this system, in both the condensed and gas phases, was thoroughly investigated here. Moreover, the influence of the addition of an ultrasonication step, between each deposition step, was evaluated to see if it altered the FR mechanism. A unique "microintumescent" mechanism, acting in both the condensed phase and the gas phase at the cotton surface, was revealed in this study. This new understanding should help researchers to further improve the FR behavior of these important nanocoatings.

EXPERIMENTAL

Chemicals and Substrates

CH ($M_w \cong$ 60,000 g/mol, G.T.C. Bio Corporation, Qingdao, China), ammonium polyphosphate (APP-AP422, Clariant), branched polyethylenimine (BPEI) ($M_w \cong$ 25,000 g/mol, Aldrich, St. Louis, MO), hydrochloric acid (HCl) (ACS reagent 37%, Aldrich), and sodium hydroxide (NaOH) (ACS reagent > 97.0%, Aldrich) were used as received. Desized, scoured, and bleached plain-woven cotton fabric, with a weight of 100 g/m^2, was purchased from Testfabrics, Inc. (West Pittston, PA). Silicon wafers (single-side-polished (100), University wafer, South Boston, MA) and polished Ti/Au crystals (Maxtek, Inc., Cypress, CA), with a resonance frequency of 5 MHz, were used for characterization of film growth.

Layer-by-Layer Deposition and Film Growth

Separate 1 wt % AP422 (pH 4.2) and 1 wt % BPEI (unmodified pH) solutions were prepared in deionized water (18.2 MΩ). A 0.5 wt % CH solution was prepared in pH 1.5 HCl solution and then adjusted to pH 4 using 1 *M* NaOH. A 5 min plasma cleaning treatment, using a PDC-32G plasma cleaner (Harrick Plasma, Ithaca, NY), was performed on quartz crystals prior to deposition. All film growth began with a 5 min deposition of BPEI solution to improve adhesion to the substrates. Films were then alternately dipped between the anionic APP and cationic CH solutions, beginning with APP. The first dip into APP was 5 min, while the rest of the deposition steps was 1 min. The fabric (or other substrate) was rinsed in DI water for 1 min between every deposition. The fabric was wringed out by hand after each deposition and rinse step to remove excess liquid. After the desired number of bilayers was deposited, samples were dried in a 70 °C oven for 2 h. Ti/Au crystals were dried using a stream of dry air after each rinse step to minimize moisture uptake. For the sonication procedure, fabric was rinsed for 1 min in a 10 L Branson 5510 ultrasonic cleaner (Branson Ultra-sonics Corporation, Danbury, CT). Rinse water was replaced after every five bilayers of deposition. Mass deposited was measured on Ti/Au crystals using a Maxtek Research quartz crystal microbalance (QCM) from Infinicon (East Syracuse, NY), with a frequency range of 3.8–6 MHz.

Morphological and Chemical Analyses

The raw and treated cotton fibers were observed before and after burning using a Hitachi S4700 Scanning Electron Microscope (SEM), at an accelerating voltage of 6 kV and a current of 10 μA. Chemical composition of samples was evaluated with a CAMECA SX100 Electron Probe Microscopy Analysis (EPMA) tool. Some samples were analyzed in cross-section by embedding them into an epoxy resin, followed by polishing (up to 0.25 μm) and carbon coating with a Bal-Tec SCD005 sputter coater. Backscattered electron (BSE) images were obtained at 15 kV and 15 nA. In BSE images, the darkest parts correspond to the "lightest" elements. Low- and high-magnification images were taken in various parts of the samples to have a representative picture. Phosphorus X-ray mapping was carried out at 15 kV and 40 nA. Elemental analysis was performed by an external laboratory (Institut des Sciences Analytiques, CNRS, Villeurbanne-FRANCE) to evaluate the weight percentage of phosphorus and nitrogen in the samples. The quantity of nitrogen was determined by burning the sample in He, containing 3% O_2, at 1050 °C. The evolved nitro-generated oxides were then reduced to molecular nitrogen, the quantity of which was determined with a catharometer. The quantity of phosphorus was determined by mineralization in aqueous media and plasma emission spectrometry. Solid-state ^{31}P NMR measurements were performed using a Bruker Avance 400 spectrometer to identify phosphorus containing species in CH-APP treated cotton, before and after burning (with and without sonication). Bruker probe heads equipped with a 4 mm magic angle spinning (MAS) assembly were used. The experiments were carried out at 162 MHz (16 scans, 120 s relaxation delay, 2.5 μs pulse length, and 10 kHz spinning rate). An H_3PO_4 aqueous solution (85%) was used as reference.

Fire Testing

Vertical flame testing (VFT) was performed on five 50 × 100 mm fabric samples according to ASTM D 6413, by applying a propane flame for 10 s at the bottom of the fabric specimen. The test was repeated three times for each formulation to ensure repeatability of results. A mass loss calorimeter (MLC, Fire Testing Technology [FTT], West Sussex, UK) was used to carry out measurements on cotton samples following the ASTM E 906 procedure. The equipment is similar to the one used in oxygen consumption cone calorimetry (ASTM E-1354-90), except that a thermopile placed in the chimney is used to obtain heat release rate (HRR) instead of employing the oxygen consumption principle. Cotton samples (100 mm^2) were exposed in a horizontal orientation. They were covered by a grid to prevent bending and then placed in aluminum foil, leaving the upper surface exposed to the heater (external heat flux 35 kW/m^2), and finally placed on a ceramic backing board at a distance of 25 mm from cone base. The mass loss calorimeter allows determining the following main fire properties: HRR as a function of time, peak of heat release rate (pHRR), time to ignition (TTI), and total heat release (THR). When measured at 35 kW/m^2, HRR, THR, and TTI values are reproducible to within ± 10%. Experiments were performed three times to ensure repeatability.

Thermal Analyses

The thermal stability, degradation temperature, and pyrolysis behavior of cotton was measured with a Q5000 Thermogravimetric Analyzer (TGA) (TA Instruments, New Castle, DE). Each sample was approximately 10 mg and tests were conducted in nitrogen, from room temperature to 800 °C, with a heating rate

of 10 °C/min. All tests were conducted in triplicate. Microscale combustion experiments were conducted with an FTT microscale combustion calorimeter (MCC), following ASTM D 7309. Each sample was approximately 7 mg and the test was performed under a nitrogen atmosphere with a heating rate of 1 °C/s, from 150 to 750 °C. MCC provided the pHRR, measured in W/g. All experiments were repeated in triplicate.

Gas Phase Analyses

Gases released during the MLC experiment were analyzed with a Fourier transform infra-red spectrometer (MLC-FTIR). This device allows the online analysis of released gases quantitatively and qualitatively. The gas picking pistol and transfer line were provided by M&C Tech Group (Germany), and the Antaris™ Industrial Gas System (i.e., FTIR), was provided by Thermo-Fisher. The transfer line between the MLC and FTIR is 2 m long and was heated up to 200 °C. Two temperature controllers were installed to ensure a constant temperature in the transfer line. Before analyzing the gases by FTIR, soot particles were filtered off by two different heated filters (2 and 0.1 mm), consisting of glass fibers and ceramic, respectively. The FTIR gas cell was set to 185 °C and 652 Torr. The optical pathway is 2 m long and the chamber of the spectrometer is filled with dry air. FTIR spectra obtained using (MLC-FTIR) were treated using OMNIC software. To quantify gases, a quantification method already developed was used.[57] MLC-FTIR allows the following gases to be quantified: water, carbon monoxide, carbon dioxide, aldehyde, acetic acid, ammonia, methane, nitrogen monoxide, nitrogen dioxide, and hydrogen cyanide. Quantification is reproducible within ± 10%. Each experiment was performed two times to ensure repeatability.

Pyrolysis-GC/MS is an accurate tool to identify the nature of gases released during the thermal decomposition of a material and its utility to elucidate FR mechanisms has been proven many times.[57,58] The system used was purchased from Shimadzu (Tokyo, Japan) and has a Frontier Lab PY-2020iD micro-furnace pyrolyzer (Fukushima, Japan), a gas chromatograph (equipped with a capillary column), and a quadrupole mass spectrometer [equipped with an Electron-Impact (EI) ionization source (Shimadzu GC/MS QP2010 SE)], all directly connected in series. Sample (0.2 mg) is put in a stainless-steel sample cup. This cup is first placed at the upper position of the pyrolyzer, and further introduced into the center of the furnace (inside a quartz tube vial) under a helium gas flow. In the pyrolyzer furnace, the temperature was initially set at 50 °C and a 10 °C/min ramp was programmed up to 800 °C. The temperature of the interface between the pyrolyzer and the GC injection port was set at 320 °C, and the temperature between the column and the mass spectrometer was set at 280 °C. A fused silica capillary column (30 mm × 0.25 mm × 0.25 μm film thickness) was used with helium as the carrier gas with a linear velocity of 40 cm/s. The GC column temperature was maintained at 35 °C for 80 min (during the ramp and followed by a 5 min isotherm) and then heated up to 300 °C at a rate of 5 °C/min, followed by an isotherm at 300 °C of 10 min. With this program, the studied cotton samples were treated the same as during the TGA, while volatile compounds were observed, and then the heavier compounds were desorbed from the column during its temperature ramp. Electron-Impact spectra were recorded at 85 eV with a mass scan rate of 2 scan/s. The data obtained were treated using a GC/MS post-run analysis program (Shimadzu). Products were identified using the NIST and FSearch mass spectral databases.

RESULTS AND DISCUSSION

Film Growth

Mass growth was registered as a function of bilayer deposition of APP and CH, as monitored by a quartz crystal microbalance. The film mass increases linearly (Supporting Information, Figure S1) with increasing bilayers, as opposed to sodium polyphosphate–CH assemblies, which deposit in a supralinear manner.[34] It is possible that the long-chain APP molecules cover the substrate completely in the first bilayer, avoiding the island growth regime entirely.[59] The rigidity of both molecules likely contributes to reduced interdiffusion that contributes to this linear growth.

Morphology before Burning

Figure 1 shows the SEM surface images of the three types of cotton samples. Without sonication, aggregates of polyphosphates and CH are present mostly at the surface of the fabric [Figure 1(b)], gluing individual fibers together. Sonication prevents formation of phosphorus containing aggregates at the fabric surface [Figure 1(c)] and allows the polyelectrolytes to penetrate deeper into the fabric (through the fibers), so the fabric looks much more like uncoated cotton [Figure 1(a)]. This can explain why ultrasonication rinsing significantly improves the hand of the fabric, as was recently demonstrated.[34] With or without sonication, surface fibers are uniformly covered with the CH–APP assembly. This difference of deposition mode (one is a thick surface coating with untreated cotton fibers deeper inside, while the other one is more uniformly distributed throughout the fabric) does not play a significant role in the FR behavior of the cotton, as will be shown below. Single fibers of each fabric without [Figure 1(f)] and with [Figure 1(g)] sonication were analyzed by SEM at higher magnification. Both 20 BL treatments result in fully and homogeneously coated fibers, with the assembly similar to LbL coatings on a previously studied polyester–cotton fabric.[60]

Elemental analysis was also conducted on the cotton with and without a CH-APP treatment (with and without sonication during treatment). The nonsonicated coated sample contains 1.31% phosphorus and 0.56% nitrogen [Figure 1(d)], while the sonicated cotton contains only 0.90% phosphorus and nearly the same amount of nitrogen (0.59%) [Figure 1(e)]. Microscopy was used to determine if these differences correlate with the deposition morphology. The relative amounts of phosphorus on the fabric surfaces were compared using phosphorous X-ray mapping [color scales are the same in both Figure 1(d,e)]. Phosphorus-containing species are present in high concentration on the nonsonicated fabric surface, both on and between the fibers. The sonicated fabric has a lower amount of phosphorus, but it is more homogeneously deposited on and around the fibers. As the LbL deposition was carried out by dipping, it was assumed that the coating would penetrate deeply inside the fabric. To verify this assumption, cross-sectional SEM images of

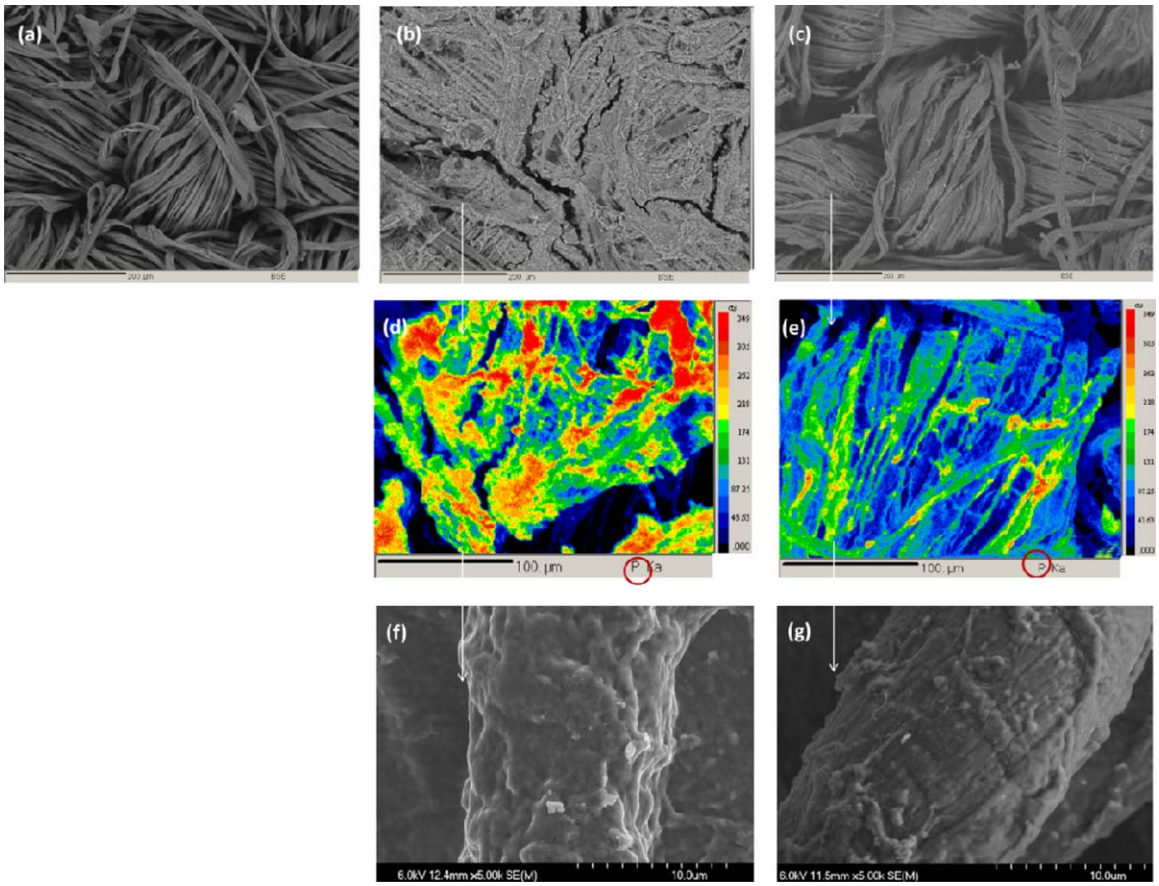

Figure 1. EPMA-BSE image of (a) uncoated cotton fabric, (b) nonsonicated 20 BL APP-CH cotton fabric, and (c) sonicated 20 BL APP-CH cotton fabric. EPMA-phosphorus X-ray mapping of (d) nonsonicated APP-CH cotton fabric and (e) sonicated APP-CH cotton fabric, along with SEM images of the (f) nonsonicated and (g) sonicated fabric. [Color figure can be viewed in the online issue, which is available at wileyonlinelibrary.com.]

the fabrics were obtained. Only the most representative pictures (i.e., the phosphorus cross-section X-ray mapping) are shown in Figure 2. On the nonsonicated sample [Figure 2(a)], the coating is clearly visible, with a large amount of phosphorus on each side of the fabric cross-section, but the amount of phosphorus inside the fabric is very low. It appears that the coating does not easily penetrate inside the fabric. It is possible that aggregation on the surface of the fabric prevents deeper penetration of the coating into the textile. This image suggests that the APP-CH treatment without sonication leads to a thick surface coating, with uncoated cotton fibers deeper inside the fabric. The sonicated sample [Figure 2(b)] is quite different, showing that phosphorus is present in a larger amount inside the fabric, whereas it is less visible at the surface. There are now few (if

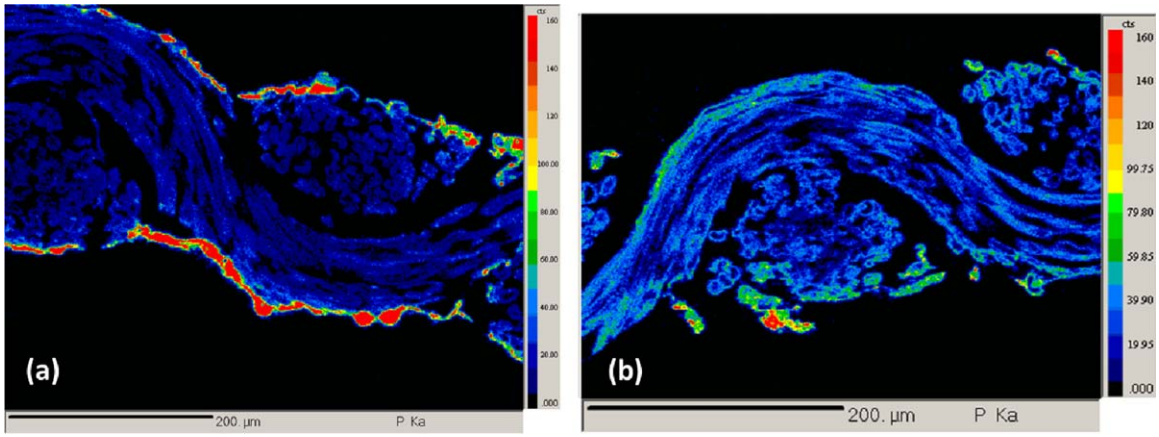

Figure 2. Cross-sectional phosphorus X-ray mapping of (a) nonsonicated and (b) sonicated cotton fabric coated with 20 APP-CH bilayers. [Color figure can be viewed in the online issue, which is available at wileyonlinelibrary.com.]

(1)

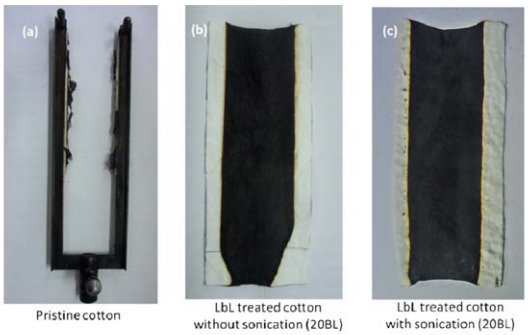

(2)

Sample	Burning Time (s)
Neat cotton	13 ± 2 s
Non-sonicated APP-CH cotton (20BL)	5 ± 1 s
Sonicated APP-CH cotton (20BL)	7s ± 2s

Figure 3. (1) Images of (a) uncoated, (b) nonsonicated, and (c) sonicated cotton fabric, following VFT. The coated fabric contained 20 BL of CH-APP. (2) Burning time results for uncoated, nonsonicated, and sonicated cotton fabric coated with 20 BL of CH-APP. [Color figure can be viewed in the online issue, which is available at wileyonlinelibrary.com.]

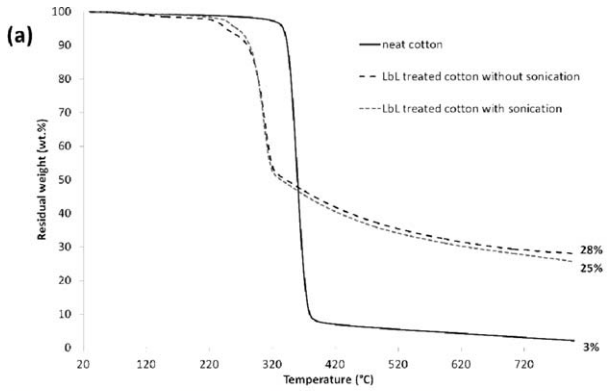

(b)	T max $_1$ (°C)	Char residue at Tmax$_1$ (wt.-%)	T max $_2$ (°C)	Char residue at Tmax$_2$ (wt.-%)	Char residue at 800°C (wt.-%)
Neat Cotton	--	--	358	49%	3%
Non sonicated APP-CH cotton	244	95%	310	64%	28%
Sonicated APP-CH cotton	251	97%	307	66%	25%

Figure 4. (a) Residual weight as a function of temperature for uncoated, nonsonicated, and sonicated cotton containing 20 BL of CH-APP. These curves were obtained with TGA, in a nitrogen atmosphere, with a heating rate of 10 °C/min and (b) related thermogravimetric data of uncoated, nonsonicated, and sonicated cotton fabric tested in a nitrogen atmosphere, with a heating rate of 10 °C/min. [Color figure can be viewed in the online issue, which is available at wileyonlinelibrary.com.]

any) surface aggregates, which was confirmed by the surface phosphorus X-ray mapping of the sonicated sample [Figure 1(e)], where a lower amount of phosphorus was visible compared to the nonsonicated sample [Figure 1(f)].

The nonsonicated and sonicated LbL-treated cotton were further analyzed by 31P solid-state NMR (Supporting Information, Figure S2 and Table S1).

The spectra of both samples are quite similar, showing Q0 units (phosphoric acid), Q1 units (pyrophosphates), and Q2 units (polyphosphates). It is interesting to note that when APP is dissolved in the conditions detailed in the Experimental (Section 2), not only are polyphosphates acquired, but also phosphoric acid and pyrophosphates. In the case of the sonicated sample, the Q0 units are relatively small compared to Q1 and Q2 units. This could be due to the fact that phosphoric acid is removed by the ultrasonic rinsing.

Flame-Retardant Behavior

The FR properties of uncoated, nonsonicated, and sonicated cotton samples were measured using a vertical flame test that characterizes the ignitability of the samples in the presence of a flame. Pictures of the tested (i.e., burned) samples are shown in Figure 3(1) and the flammability data are summarized in Figure 3(2). Unlike pristine cotton, the fabric coated with 20 bilayers of CH-APP was partially protected, as indicated by the residues shown in Figure 3(1b,1c). No particular differences are observed between the nonsonicated and sonicated samples. In both cases, a coherent residue is formed during the combustion, indicating that the assemblies are capable of protecting the cotton from flame. As shown in Figure 3(2), the burning time was significantly reduced when cotton was protected by the assembly, with slightly more heterogeneous results for the sonicated fabric.

To evaluate a realistic fire scenario, the combustion behavior under irradiative heat flow (developed as a consequence of exposure to flame) was evaluated using mass loss calorimetry. Time to ignition (TTI), time of flameout (ToF), and residual weight are presented in Supporting Information, Table S2. As the samples ignite very rapidly when put under the cone heater, the pHRR results are not reliable, so they are not presented here. It may be surprising to see that the time to ignition is reduced in the presence of the LbL coatings (both sonicated and nonsonicated). Neat cotton ignites after 11 s exposure, whereas the nonsonicated and sonicated cotton ignites after 7 and 5 s, respectively. Even so, the coated cotton stops burning very quickly, with a total burning time of 5 s for nonsonicated and 6 s for sonicated cotton. The uncoated cotton burns for 24 s. Residual weights obtained are quite high for the coated samples, while uncoated cotton is consumed almost completely by the fire [Figure 3(1a)]. It can be concluded that only a minimal amount of FR additive is needed at the fabric surface to protect the underlying fibers from further degradation in presence of a flame.

The thermal stability of the system was investigated by thermogravimetric analysis (TGA) under pyrolysis conditions, as ignition is very quick and it is reasonable to assume that oxygen is depleted in presence of the flame. Figure 4(a) shows the weight loss of cotton samples as a function of temperature in a nitrogen environment. Figure 4(b) summarizes the degradation temperatures and corresponding weight loss of uncoated cotton and the LbL-treated fabric. It is well known that pristine cotton degrades in one step near 358 °C.[61] This one-step degradation is the result of the depolymerization of the glycosyl units into

volatile products (containing levoglucosan), leading to an aliphatic char. The cotton used in this study yields 3% residue at 800 °C.

The deposition of CH-APP coatings, with and without sonication, leads to a decomposition process in two steps. The first step yields a char residue of 95% at 244 °C for the nonsonicated cotton and 97% at 251 °C for the sonicated one. This step probably corresponds to a dehydration step due to the water entrapped within the assemblies or adsorbed by CH. The second degradation step occurs at a much lower temperature relative to pristine cotton (310 and 307 °C relative to 358 °C for uncoated cotton). This phenomenon has been reported in the literature.[43] In this case, it can be attributed to the presence of hydroxyl groups in the CH molecule and the presence of phosphate groups in the APP that catalyze the dehydration reaction of cellulose toward formation of an aromatic char. This char evolves into a thermally stable structure that acts as a barrier to limit heat transfer to the substrate. It is also possible that ammonia attack could decrease the decomposition temperature, similar to phosphorus, but there is no experimental proof for this mechanism. Cotton burns completely in the absence of a coating, whereas in these pyrolysis conditions, coated cotton produces char residue of 28% (no sonication) and 25% (sonication). It should be noted that the char residue percentages are very similar to the remaining masses obtained during mass loss calorimeter measurements (Supporting Information, Table S2). This implies that the fraction of char formed is independent of the sample's heating history, suggesting that this sample is behaving as a thermally thin material. The char is formed in a single-step, noncompetitive scheme and is thermally stable.[62]

Samples were also analyzed with microscale combustion calorimetry (MCC), also known as pyrolysis combustion flow calorimetry (PCFC). Using this technique, the gases released during the pyrolysis are evacuated into an oven at 900 °C in the presence of an 80/20 N_2/O_2 mixture. In these conditions, the total combustion of these gases takes place. The HRR is determined through the measured consumption of oxygen. When correlated with TGA results, it can provide some useful information on a potential gas phase or condensed phase FR mechanism. Figure 5 shows the MCC curves obtained for the various cotton samples. Uncoated cotton degrades at 350 °C, producing a pHRR of 293 W/g. Both LbL-treated cotton samples degrade earlier, at 283 and 282 °C for nonsonicated and sonicated fabric, respectively. These coated samples also exhibit a much smaller pHRR. The pHRR of the nonsonicated cotton is reduced to 63 W/g corresponding to an 80% decrease compared to pristine cotton, whereas the sonicated one reaches 90 W/g, corresponding to a decrease of approximately 70%. This large pHRR reduction might indicate that the fire protective mechanism is gas phase,[63] but MCC results first have to be compared with TGA results. The second degradation step observed by TGA for the coated samples corresponds to the HRR peak obtained by MCC. It should be noted that the weight loss is much lower for coated samples than for raw cotton, so the mechanism of action in this case could involve the release of a large amount of gas or a condensed phase mechanism, with only a very small amount of gas released.

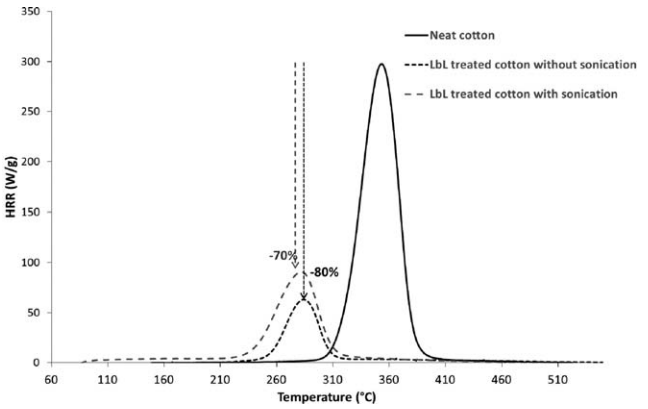

Figure 5. Heat release rate as a function of temperature, as measured by MCC, for three types of cotton samples. LbL-treated cotton contains 20 CH-APP bilayers.

Following vertical flame testing, surface, and cross-sectional SEM images of the fabric residues were analyzed. Morphologies of uncoated and treated cotton, with and without ultrasonication, are shown at various magnifications in Figure 6. Most of the uncoated cotton burned completely without leaving any residue [Figure 3(1a)], so residual fibers from next to the sample holder were analyzed [Figure 6(a,d,g)]. These residual fibers were thin and broke easily. The nonsonicated LbL-treated cotton fabric displayed a completely different surface, showing swollen fibers [compared to their initial dimensions in Figure 1(b)] and these large fibers created a smooth and homogeneous protective layer at the textile surface. This is particularly obvious in Figure 6(b), a cross-sectional view showing an outer crust that protects the cotton fibers [Figure 6(e)]. The fibers underneath this layer have combusted and are completely hollow. Under heat, lumen of cotton fibers expands, leading to these hollow tubes.[64]

Figure 6 provides the evidence that the mechanism of action is largely limited to the external layers of the cellulosic fibers. In other words, only the surface is affected by the flame, with the underlying cotton fibers remaining intact. It confirms the role of the protective film on the surface of the fibers that, by reaction with the cellulose during the pyrolysis, promotes the formation of char that will limit the amount of volatiles entering the gas phase. A surface fiber was investigated after burning using SEM at higher magnification [Figure 6(h)]. In this image, the formation of intumescent-like micro bubbles is observed that produce the expanded charred structure observed in Figure 6(b). Similar bubbles were observed with a phosphonated oligoallylamine LbL system applied to cotton.[43] In that study, the formation of the bubbles was attributed to the release of ammonia entrapped in the charred cotton structure.

The sonicated, coated fibers exhibit a different surface structure, following vertical flame testing [Figure 6(c)], than either the uncoated cotton [Figure 6(a)] or the nonsonicated LbL-treated fabric [Figure 6(b)]. No particular swelling is observed, instead the surface fibers appear smooth and homogeneous. From the cross-section [Figure 6(f)], the upper surface fibers appear to protect the underlying fibers, as was the case for the nonsonicated fabric. Similarly, hollow fibers can be observed due to the

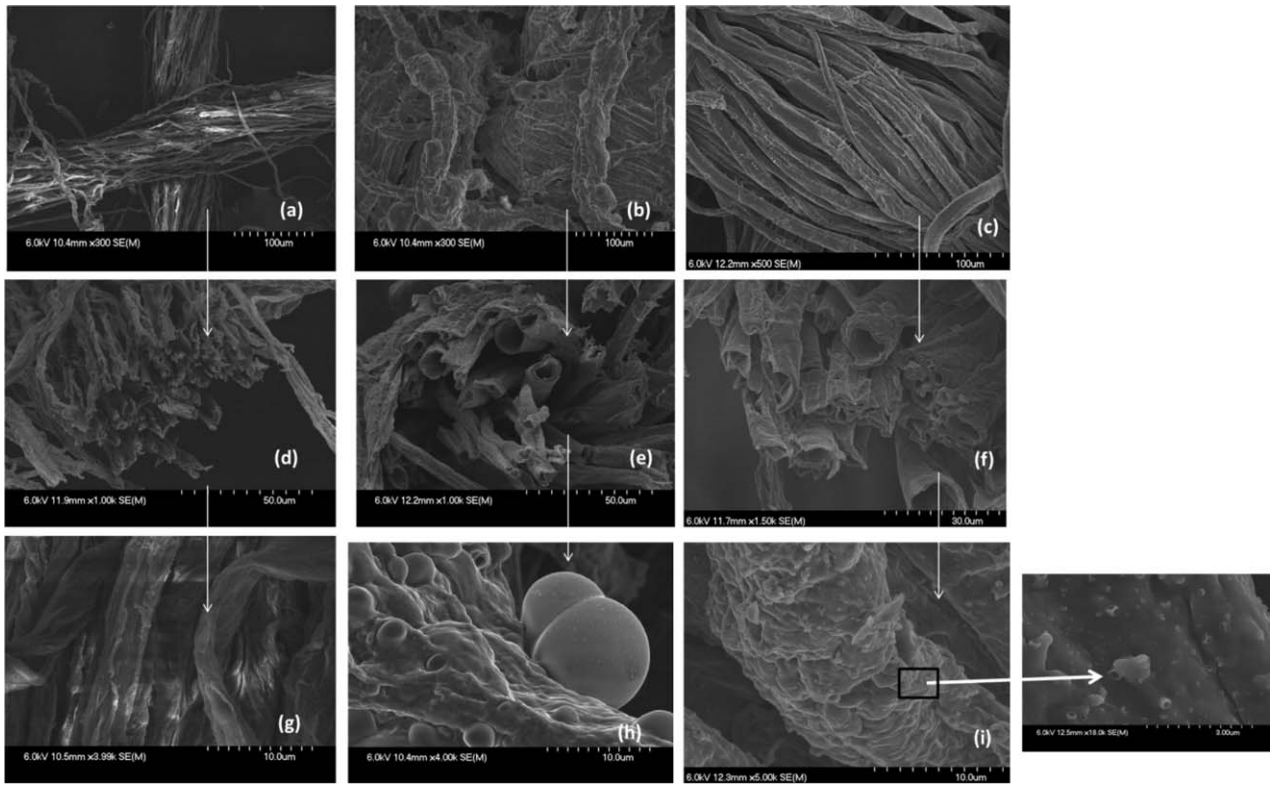

Figure 6. Surface SEM images of (a) burned uncoated cotton, (b) burned nonsonicated cotton with 20 BL of CH-APP, and (c) burned sonicated cotton with 20 BL of CH-APP. Cross-sectional SEM images of (d) burned uncoated cotton, (e) burned nonsonicated cotton with 20 BL of CH-APP, and (f) burned sonicated cotton with 20 BL of CH-APP, with high-magnification images of the same samples in (g), (h), and (i), respectively. A higher magnification of (i) is provided to show microbubbles at the sample surface.

lumen opening under heating. In contrast to the nonsonicated sample, no bubbles can be seen on the fiber surface [Figure 6(i)], but at higher magnification, there are some nano-sized surface bubbles. This difference can be ascribed to the difference in coating thickness between sonicated and nonsonicated fabric.[43] The nonsonicated coating is much heavier (i.e., thicker), with significant aggregation present [Figure 1(b)], relative to the sonicated cotton [Figure 1(c)].

In an effort to better compare the LbL-treated fabric surfaces (without and with ultrasonication) after burning, phosphorus X-ray mapping was performed, as shown in Supporting Information, Figure S3. The color intensities are directly comparable, making it obvious that phosphorus is spread everywhere after burning and in relatively high concentration on the nonsonicated sample. Phosphorus is present, but in much smaller concentration on the sonicated fabric, and it is less homogeneously distributed. It is interesting to note that fire testing shows little difference in terms of burning time between these two samples despite the sonicated fabric containing significantly less FR.

Gas Phase Analysis

The gases released during the combustion of the cotton were analyzed by an FTIR analyzer coupled to a mass loss calorimeter. Water (3951–3914 cm^{-1}), carbon dioxide (3702–3692 cm^{-1}), carbon monoxide (2049–2140 cm^{-1} and 2013–2092 cm^{-1}), and formaldehydes (2600–3200 cm^{-1}) were the primary degradation products identified, as shown in Figure 7. Results obtained for nonsonicated and sonicated cotton are very similar. Water was released very quickly and in high concentration by the LbL-treated cotton, with a maximum release at 12 s, corresponding to the time of flameout of the sample in MLC testing (Supporting Information, Table S2). The uncoated cotton also started releasing water, with a maximum amount released after 30 s, but the release rate is much slower than the coated samples. The coated samples release twice the maximum amount of water. Coated samples also released a much higher amount of carbon monoxide and a lower amount of carbon dioxide than the uncoated cotton, indicating incomplete combustion. Polyphosphates promote dehydration of both CH and cellulose fibers, thus changing the decomposition pathway of the cotton, leading to the rapid formation of char. This altered decomposition process is believed to result in incomplete combustion and a higher amount of carbon monoxide release. In the case of untreated cotton, the CO release is very low and the CO_2 release very high, which signifies complete combustion. It is believed that these samples are thermally thin, suggesting that the char is formed in a single-step, noncompetitive scheme and is thermally stable. The criterion for ignition of thermally thin materials is that of a critical mass flux of volatiles from the solid into the gas phase. This criterion is confirmed for these LbL-treated samples, as a high concentration of volatiles is released as soon as the sample is exposed to heat during MLC,

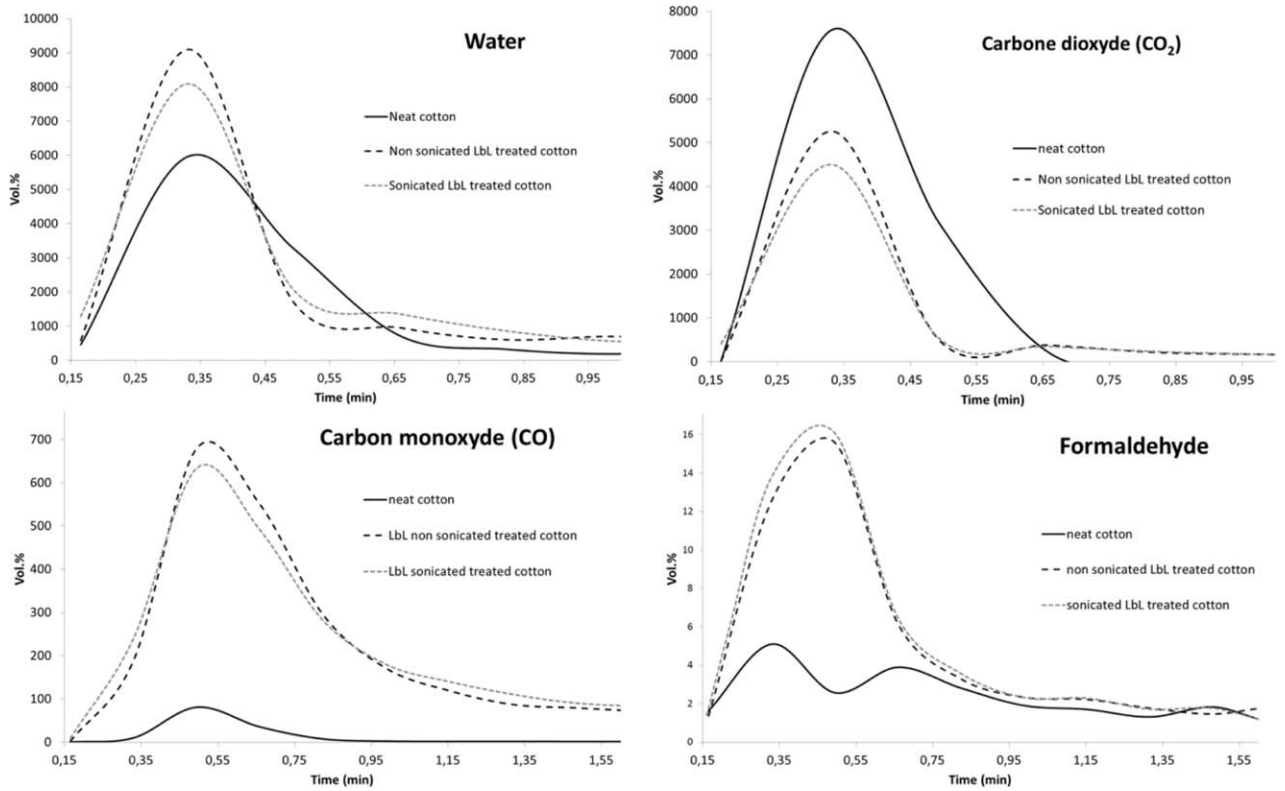

Figure 7. Quantitative FTIR measurements of water, carbon dioxide, carbon monoxide, and formaldehydes released during mass loss calorimeter testing, at 35 kW/m^2 and 25 mm, on uncoated cotton, nonsonicated cotton treated with 20 BL of CH-APP and sonicated cotton treated with 20 BL of CH-APP.

leading to a very quick ignition. It is also known that for these thermally thin materials, the major mechanism by which char formation reduces flammability is through the reduction of volatiles entering the gas phase.[62] When the treated sample stops burning, the emission of volatiles also decreases drastically. The high amount of CO released by the LbL-treated fabric proves the incomplete combustion of the sample, contrary to the pristine cotton that releases more carbon dioxide than carbon monoxide.

Formaldehyde was also identified as degradation product from the LbL-treated cotton. Its release starts before ignition, as soon as the sample is put under the cone. As it is a highly flammable gas, it can explain why the coated samples burn so quickly when exposed to the heating source. Surprisingly, no ammonia was detected. It was assumed that some ammonia would be released during combustion due to the presence of APP. This result was confirmed by TGA-FTIR (not shown) and py-GC/MS analysis, shown in Figure 8. When APP is dissolved in water and adjusted to pH 4.2 (using HCl), the ammonium ions likely react with chlorides to form ammonium chloride that remains in the deposition solution. Ammonium chloride could also deposit on cotton, but would likely be released in water during the rinsing step. It is also possible that ammonium ions are present on the fabric, but react with ether bonds of the cellulose molecules to yield pyridine or pyrrole-type structures of aromatic phosphate esters.[65,66] This last hypothesis is the most probable and was confirmed by XPS analysis (Supporting Information, Figure S5). Two bands at 401.5 and 399.7 eV are observed, corresponding to NH_4^+ groups and nitrogen in pyrrole and/or pyridine-type structures, respectively.[66] Additionally, it was recently shown that same products are also produced during the degradation of CH,[67] so it is not possible to absolutely confirm this hypothesis.

The py-GC/MS chromatogram of uncoated (pristine) cotton exhibits three primary regions. Two broad peaks are observed at 30 and 34 min, corresponding to water/CO_2/formaldehyde and furfural, respectively. These are volatiles observed during the temperature ramp (i.e., they are not retained by the column). Between 80 and 100 min, many cellulose fragments are observed. The main fragment is 2-hydroxy-6,8-dioxabicyclo-(3,2,1)-octan-4-one at 99 min, which is released during dehydration of cellulose. Between 100 and 140 min, oligomers of cellulose are observed, with a major broad peak between 100 and 110 min that corresponds to levoglucosan. The py-GC/MS chromatogram of LbL-treated cotton reveals the same three zones, but each of the zones is quite different. The initial bands are observed at shorter time, in a range between 15 and 35 min. Three peaks are observed, corresponding to water, formaldehyde/water/CO_2, and furfural. In the second and third time ranges, the most intense peak at 87 min corresponds to levoglucosenone, which is from strong dehydration of cellulose.

Water is also released in high amount soon after the beginning of the experiment, and the time corresponding to the maximum water release is well correlated to the time of flame extinction. The addition of APP causes a strong dehydration of CH and cotton's cellulose chains. Both the presence of hydroxyl groups

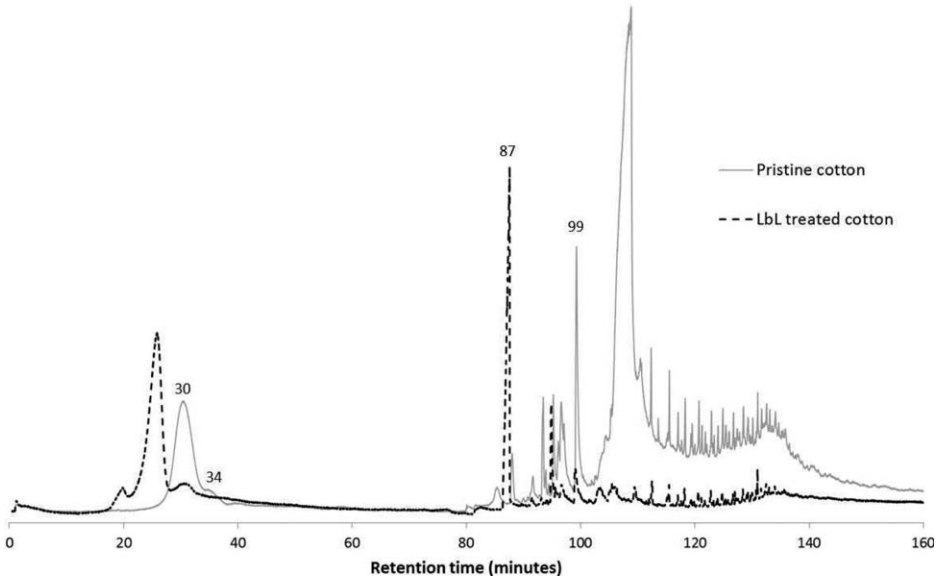

Figure 8. Py-GC/MS chromatograms of pristine cotton and LbL-treated cotton containing 20 BL of CH-APP nanocoating.

in the CH molecule and in cotton, combined with the presence of phosphate groups, can catalyze a dehydration reaction of cellulose toward formation of an aromatic char. The presence of levoglucosenone instead of levoglucosan (Supporting Information, Figure S6) is another key observation to support this hypothesis. The fire protective mechanism established, summarized in Figure 9, is that the presence of polyphosphates promotes dehydration of CH and cellulose fibers at the surface of the fabric, leading to a rapid degradation of the LbL coating (evolving both highly flammable formaldehyde and water that extinguishes the flame). This process forms an aromatic protective char primarily composed of levoglucosenone, phosphoric acid, and pyridine or pyrrole-type structures of aromatic phosphate esters. The gases released are trapped in small concentration in the charring burning layer, promoting a kind of "microintumescence" phenomenon. Acetic acid, methane, and ethane may have been expected decomposition products, but none of these molecules were detected by any of the analysis performed in this study.

CONCLUSIONS

A 20 bilayer CH-APP nanocoating was applied on cotton fabric, using LbL deposition, and tested for flammability (VFT and MLC). Both sonicated and nonsonicated samples appear to significantly reduce cotton flammability. A combination of both condensed and gas phase mechanisms at the cotton surface appears to be the reason for the effective FR properties of this CH-APP LbL coating. The fire protective mechanism established is that the presence of polyphosphates promotes dehydration of CH and cellulose fibers at the surface of the fabric, leading to a rapid degradation of the LbL coating, evolving both highly flammable formaldehyde and water that extinguishes the flame. This process forms an aromatic protective char at the fabric surface, primarily composed of levoglucosenone, phosphoric acid, and pyridine or pyrrole-type structures of aromatic phosphate esters that protect the underlying cotton fibers. The gases released are trapped in small concentration in the charring burning layer, promoting a kind of "microintumescence"

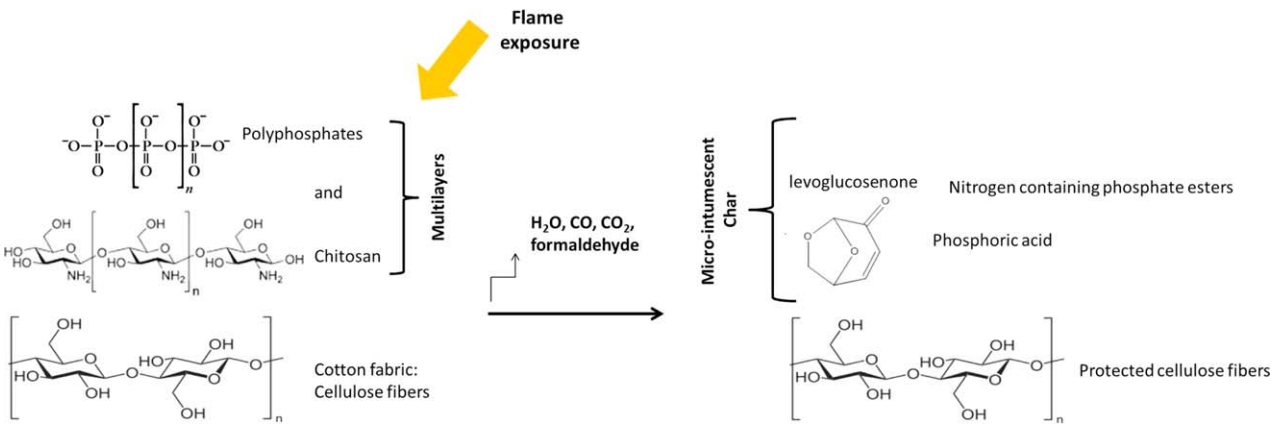

Figure 9. Flame-retardant mechanism of action for the APP-CH LbL treatment of cotton fabric. [Color figure can be viewed in the online issue, which is available at wileyonlinelibrary.com.]

phenomenon. This FR mechanism is not affected by ultrasonication of the cotton fabric between each deposition step, even though the coatings are different. CH-APP treatment without sonication does not easily penetrate inside the fabric and leads to a thick surface coating, with uncoated cotton fibers deeper inside the fabric. It is possible that aggregation on the surface of the fabric prevents deeper penetration of the coating into the textile. The sonicated sample is quite different, showing that phosphorus is present in a larger amount inside the fabric, whereas it is less visible at the surface.

Fire testing shows little difference in terms of burning time between sonicated and nonsonicated samples, despite the sonicated fabric containing significantly less fire retardants at the surface. This means that this system effectively protects cotton fabric against fire, even at low FR surface concentration. This means that the same result might be obtained by applying only a few bilayers, thus reducing chemicals and processing time. An aqueous polyelectrolyte complex (PEC) of nitrogen poly(ethylenimine) and phosphorous-rich (polysodium phosphate) species, similar to those studied here, have recently been shown to self-extinguish cotton in just two processing steps.[68] As noted above, there are promising routes to reduce the number of processing steps for LbL-deposited coatings. LbL deposition tends to produce a more conformal coating and a wider variety of ingredients can be used relative to these newer PEC-based coatings. Both technologies offer the opportunity for effective, environmentally benign FR treatment for cotton (and other polymeric substrates).

ACKNOWLEDGMENTS

JCG and TG acknowledge the Texas A&M Engineering Experiment Station (TEES) for infrastructural support of this work. The authors also acknowledge Me Martine Trentesaux (Plateforme Régionale d'analyse des Surfaces, Université Lille Nord de France) for the XPS analyses and M. Bertrand DOUMERT (Fédération Chevreul) and M. Bertrand REVEL for solid-state NMR analyses.

ABBREVIATIONS

APP	ammonium polyphosphate
BL	bilayer
BPEI	branched polyethylenimine
CH	chitosan
EPMA	electron probe microanalysis
FR	flame retardant
FTIR	Fourier transform infrared spectroscopy
GC/MS	gas chromatography – mass spectrometry
HRR	heat release rate
LbL	layer-by-layer
MCC	micro cone calorimetry
MLC	mass loss calorimetry
NMR	nuclear magnetic resonance
QCM	quartz crystal microbalance
SEM	scanning electron microscopy
TGA	thermogravimetric analysis
VFT	vertical flame test

REFERENCES

1. Chen, J. T.; Fu, Y. J.; An, Q. F.; Lo, S. C.; Huang, S. H.; Hung, W. S.; Hu, C. C.; Lee, K. R.; Lai, J. Y. *Nanoscale* **2013**, *5*, 9081.
2. Gu, C. H.; Wang, J. J.; Yu, Y.; Sun, H.; Shuai, N.; Wei, B. *Carbohydr. Polym.* **2013**, *92*, 1579.
3. Guin, T.; Krecker, M.; Hagen, D. A.; Grunlan, J. C. *Langmuir* **2014**, *30*, 7057.
4. Hagen, D. A.; Box, C.; Greenlee, S.; Xiang, F.; Regev, O.; Grunlan, J. C. *RSC Adv.* **2014**, *4*, 18354.
5. He, X.; Wu, L. L.; Wang, J. J.; Zhang, T.; Sun, H.; Shuai, N. *High Perform. Polym.* **2015**, *27*, 318.
6. Jang, W. S.; Rawson, I.; Grunlan, J. C. *Thin Solid Films* **2008**, *516*, 4819.
7. Laufer, G.; Kirkland, C.; Cain, A. A.; Grunlan, J. C. *ACS Appl. Mater. Interfaces* **2012**, *4*, 1643.
8. Priolo, M. A.; Gamboa, D.; Holder, K. M.; Grunlan, J. C. *Nano Lett.* **2010**, *10*, 4970.
9. Priolo, M. A.; Holder, K. M.; Gamboa, D.; Grunlan, J. C. *Langmuir* **2011**, *27*, 12106.
10. Priolo, M. A.; Holder, K. M.; Greenlee, S. M.; Stevens, B. E.; Grunlan, J. C. *Chem. Mater.* **2013**, *25*, 1649.
11. Priolo, M. A.; Holder, K. M.; Guin, T.; Grunlan, J. C. *Macromol. Rapid Commun.* **2015**,
12. Svagan, A. J.; Åkesson, A.; Cárdenas, M.; Bulut, S.; Knudsen, J. C.; Risbo, J.; Plackett, D. *Biomacromolecules* **2012**, *13*, 397.
13. Xiang, F.; Tzeng, P.; Sawyer, J. S.; Regev, O.; Grunlan, J. C. *ACS Appl. Mater. Interfaces* **2014**, *6*, 6040.
14. Yang, Y. H.; Haile, M.; Park, Y. T.; Malek, F. A.; Grunlan, J. C. *Macromolecules* **2011**, *44*, 1450.
15. Farias, E. A. O.; Dionisio, N. A.; Quelemes, P. V.; Leal, S. H.; Matos, J. M. E.; Filho, E. C. S.; Bechtold, I. H.; Leite, J. R. S. A.; Eiras, C. *Mater. Sci. Eng. C* **2014**, *35*, 449.
16. Gomes, A. P.; Mano, J. F.; Queiroz, J. A.; Gouveia, I. C. *Polym. Adv. Technol.* **2013**, *24*, 1005.
17. Lu, Y.; Wu, Y.; Liang, J.; Libera, M. R.; Sukhishvili, S. A. *Biomaterials* **2015**, *45*, 64.
18. Lv, H.; Chen, Z.; Yang, X.; Cen, L.; Zhang, X.; Gao, P. *J. Dent.* **2014**, *42*, 1464.
19. Zhou, B.; Hu, Y.; Li, J.; Li, B. *Int. J. Biol. Macromol.* **2014**, *64*, 402.
20. Zhou, B.; Li, Y.; Deng, H.; Hu, Y.; Li, B. *Colloids Surf. B: Biointerfaces* **2014**, *116*, 432.
21. Bae, J.; Cho, J.; Char, K. in IUMRS International Conference in Asia 2006, IUMRS-ICA 2006; Trans Tech Publications Ltd, Jeju: **2007**, p 559.
22. Geng, Z.; He, J.; Xu, L. *Mater. Res. Bull.* **2012**, *47*, 1562.
23. Li, X.; He, J. *ACS Appl. Mater. Interfaces* **2012**, *4*, 2204.
24. Li, X.; He, J.; Liu, W. *Mater. Res. Bull.* **2013**, *48*, 2522.
25. Podsiadlo, P.; Sui, L.; Elkasabi, Y.; Burgardt, P.; Lee, J.; Miryala, A.; Kusumaatmaja, W.; Carman, M. R.; Shtein, M.; Kieffer, J.; Lahann, J.; Kotov, N. A. *Langmuir* **2007**, *23*, 7901.

26. Zhang, L.; Li, Y.; Sun, J.; Shen, J. *J. Colloid Interface Sci.* **2008**, *319*, 302.
27. Apaydin, K.; Laachachi, A.; Ball, V.; Jimenez, M.; Bourbigot, S.; Toniazzo, V.; Ruch, D. *Polym. Degrad. Stabil.* **2013**, *98*, 627.
28. Apaydin, K.; Laachachi, A.; Ball, V.; Jimenez, M.; Bourbigot, S.; Toniazzo, V.; Ruch, D. *Polym. Degrad. Stabil.* **2014**, *106*, 158.
29. Apaydin, K.; Laachachi, A.; Ball, V.; Jimenez, M.; Bourbigot, S.; Ruch, D. *Colloids Surf. A: Physicochem. Eng. Asp.* **2015**, *469*, 1.
30. Laachachi, A.; Ball, V.; Apaydin, K.; Toniazzo, V.; Ruch, D. *Langmuir* **2011**, *27*, 13879.
31. Carosio, F.; Di Blasio, A.; Alongi, J.; Malucelli, G. *Polymer (United Kingdom)* **2013**, *54*, 5148.
32. Cheng, D.; Liu, X.; Wu, J.; Yu, W. *Ind. Textila* **2012**, *63*, 115.
33. Malucelli, G.; Bosco, F.; Alongi, J.; Carosio, F.; Di Blasio, A.; Mollea, C.; Cuttica, F.; Casale, A. *RSC Adv.* **2014**, *4*, 46024.
34. Guin, T.; Krecker, M.; Milhorn, A.; Grunlan, J. C. *Cellulose* **2014**, *21*, 3023.
35. Fang, F.; Zhang, X.; Meng, Y.; Gu, Z.; Bao, C.; Ding, X.; Li, S.; Chen, X.; Tian, X. *Surf. Coat. Technol.* **2015**, *262*, 9.
36. Huang, G.; Liang, H.; Wang, X.; Gao, J. *Ind. Eng. Chem. Res.* **2012**, *51*, 12299.
37. Laufer, G.; Carosio, F.; Martinez, R.; Camino, G.; Grunlan, J. C. *J. Colloid Interface Sci.* **2011**, *356*, 69.
38. Laufer, G.; Kirkland, C.; Morgan, A. B.; Grunlan, J. C. *Biomacromolecules* **2012**, *13*, 2843.
39. Laufer, G.; Li, Y. C.; Grunlan, J. C. 13th International Conference and Exhibition on Fire and Materials 2013, San Francisco, CA, **2013**, pp 611.
40. Pan, H.; Wang, W.; Pan, Y.; Song, L.; Hu, Y.; Liew, K. M. *Carbohydr. Polym.* **2014**, *115*, 516.
41. Li, Y. C.; Schulz, J.; Mannen, S.; Delhom, C.; Condon, B.; Chang, S.; Zammarano, M.; Grunlan, J. C. *ACS Nano* **2010**, *4*, 3325.
42. Carosio, F.; Alongi, J.; Malucelli, G. *Polym. Degrad. Stabil.* **2013**, *98*, 1626.
43. Carosio, F.; Negrell-Guirao, C.; Di Blasio, A.; Alongi, J.; David, G.; Camino, G. *Carbohydr. Polym.* **2015**, *115*, 752.
44. Alongi, J.; Carosio, F.; Malucelli, G. *Cellulose* **2012**, *19*, 1041.
45. Aoki, P. H. B.; Alessio, P.; Volpati, D.; Paulovich, F. V.; Riul, A.; Jr,; Oliveira, O. NJr,.; Constantino, C. J. L. *Mater. Sci. Eng. C* **2014**, *41*, 363.
46. Carosio, F.; Di Blasio, A.; Cuttica, F.; Alongi, J.; Frache, A.; Malucelli, G. *Ind. Eng. Chem. Res.* **2013**, *52*, 9544.
47. Dierendonck, M.; De Koker, S.; De Rycke, R.; De Geest, B. G. *Soft Matter* **2014**, *10*, 804.
48. Elosua, C.; Lopez-Torres, D.; Hernaez, M.; Matias, I. R.; Arregui, F. J. *Nanoscale Res. Lett.* **2013**, *8*,
49. Huang, C.; Grobert, N.; Watt, A. A. R.; Johnston, C.; Crossley, A.; Young, N. P.; Grant, P. S. *Carbon* **2013**, *61*, 525.
50. Lee, K. K.; Ahn, C. H. *ACS Appl. Mater. Interfaces* **2013**, *5*, 8523.
51. Saetia, K.; Schnorr, J. M.; Mannarino, M. M.; Kim, S. Y.; Rutledge, G. C.; Swager, T. M.; Hammond, P. T. *Adv. Funct. Mater.* **2014**, *24*, 492.
52. Shao, L.; Jeon, J. W.; Lutkenhaus, J. L. *J. Mater. Chem. A* **2014**, *2*, 14421.
53. Sung, C.; Hearn, K.; Reid, D. K.; Vidyasagar, A.; Lutkenhaus, J. L. *Langmuir* **2013**, *29*, 8907.
54. Xiang, F.; Givens, T. M.; Grunlan, J. C. *Ind. Eng. Chem. Res.* **2015**, *54*, 5254.
55. Chang, S.; Slopek, R. P.; Condon, B.; Grunlan, J. C. *Ind. Eng. Chem. Res.* **2014**, *53*, 3805.
56. Apaydin, K.; Laachachi, A.; Fouquet, T.; Jimenez, M.; Bourbigot, S.; Ruch, D. *RSC Adv.* **2014**, *4*, 43326.
57. Hoffendahl, C.; Fontaine, G.; Duquesne, S.; Taschner, F.; Mezger, M.; Bourbigot, S. *RSC Adv.* **2014**, *4*, 20185.
58. Jimenez, M.; Lesaffre, N.; Bellayer, S.; Dupretz, R.; Vandenbossche, M.; Duquesne, S.; Bourbigot, S. *RSC Adv.* **2015**, *5*, 63853.
59. Kleinfeld, E. R.; Ferguson, G. S. *Chem. Mater.* **1996**, *8*, 1575.
60. Carosio, F.; Alongi, J.; Malucelli, G. *Carbohydr. Polym.* **2012**, *88*, 1460.
61. Alongi, J.; Camino, G.; Malucelli, G. *Carbohydr. Polym.* **2013**, *92*, 1327.
62. Nelson, M. I.; Brindley, J.; McIntosh, A. C. *J. Appl. Math. Decis. Sci.* **2002**, *6*, 155.
63. Salmeia, K. A.; Fage, J.; Liang, S.; Gaan, S. *Polymers* **2015**, *7*, 504.
64. Gaan, S.; Rupper, P.; Salimova, V.; Heuberger, M.; Rabe, S.; Vogel, F. *Polym. Degrad. Stabil.* **2009**, *94*, 1125.
65. Bourbigot, S.; Le Bras, M.; Delobel, R.; Gengembre, L. *Appl. Surf. Sci.* **1997**, *120*, 15.
66. Bourbigot, S.; Le Bras, M.; Gengembre, L.; Delobel, R. *Appl. Surf. Sci.* **1994**, *81*, 299.
67. Corazzari, I.; Nisticò, R.; Turci, F.; Faga, M. G.; Franzoso, F.; Tabasso, S.; Magnacca, G. *Polym. Degrad. Stab.* **2015**, *112*, 1.
68. Haile, M.; Fincher, C.; Fomete, S.; Grunlan, J. C. *Polym. Degrad. Stabil.* **2015**, *114*, 60.

SGML and CITI Use Only
DO NOT PRINT